

**Consistently computing the  $K \rightarrow \pi$  long distance weak transition**

J. Lowe

*Physics Department, University of New Mexico, Albuquerque, NM 87131*

M.D. Scadron

*Physics Department, University of Arizona, Tucson, AZ 85721***Abstract**

First we extract the long-distance (LD) weak matrix element  $\langle \pi | H_W | K \rangle$  from  $K \rightarrow 2\pi$ ,  $K \rightarrow 3\pi$ ,  $K_L \rightarrow 2\gamma$ ,  $K^+ \rightarrow \pi^+ e^+ e^-$ ,  $K^+ \rightarrow \pi^+ \mu^+ \mu^-$  and  $K_L \rightarrow \mu^+ \mu^-$  data and give compatible theoretical estimates. We also link this LD scale to the single-quark-line (SQL) transition scale  $\beta_W$  and then test the latter SQL scale against the decuplet weak decay amplitude ratio  $\langle \pi^- \Xi^0 | H_W | \Omega^- \rangle / \langle \Xi^- | H_W | \Omega^- \rangle$ . Finally, we study LD  $K_S \rightarrow 2\gamma$  decay. All of these experimental and theoretical values for  $\langle \pi | H_W | K \rangle$  are in good agreement. We deduce an average value from eleven experimental determinations of  $\langle \pi | H_W | K \rangle = (3.59 \pm 0.05) \times 10^{-8} \text{ GeV}^2$ , while the theoretical SQL values average to  $(3.577 \pm 0.004) \times 10^{-8} \text{ GeV}^2$ .

PACS numbers: 13.20.Eb and 13.25.Es

**I. INTRODUCTION**

The weak matrix element,  $\langle \pi | H_W | K \rangle$ , appears in expressions for many kaon decay rates. Here, we deduce values for it from several experimental and theoretical sources. The work is an up-date to, and extension of, an earlier analysis [1]. Our goal is to demonstrate that there is a good deal of consistent information, both experimental and theoretical, on this matrix element, and that a reliable numerical value is available. In Sect. II, we extract four values of  $\langle \pi | H_W | K \rangle$  from data and we show that these are in good agreement with each other and with two theoretical estimates. In Sects. III and IV, we study the SQL scale,  $\beta_W$ , demonstrating consistency with values from first and second-order treatments and yielding two further values for the  $K \rightarrow \pi$  weak matrix element. In Sect. V, we derive yet another value for  $\langle \pi | H_W | K \rangle$  from the weak  $K_L \rightarrow \mu^+ \mu^-$  rate together with the electromagnetic  $\pi e \bar{e}$  and  $\eta \mu \bar{\mu}$  rates, and in Sect. VI, we demonstrate consistency of our numerical result with the parity-violating  $K_S \rightarrow \gamma \gamma$  decay. Sect. VII summarises the results.

Throughout, the work uses the current-algebra (CA) partially conserved axial current (PCAC)-consistency scheme, as was studied in Ref. [1]. Such a low-energy CA-PCAC chiral approach generates long-distance (LD) weak amplitudes for an  $H_W$  built up from  $V - A$  weak currents satisfying the charge algebra  $[Q_5 + Q, H_W] = 0$ .

Unless otherwise stated, all data in the following are taken from the Particle Data Group (PDG) tabulation [2].

## II. EXPERIMENTAL and THEORETICAL TESTS of the $K \rightarrow \pi$ WEAK SCALE

### II.1 From $K_S \rightarrow \pi\pi$ decays

CA-PCAC consistency requires amplitude magnitudes, for  $f_\pi \approx 93$  MeV [1]:

$$\begin{aligned} |\mathcal{M}_{K_S\pi\pi}^{+-}| &= \frac{1}{f_\pi} |\langle \pi^+ | H_W | K^+ \rangle| (1 - m_\pi^2/m_K^2), \\ |\mathcal{M}_{K_S\pi\pi}^{00}| &= \frac{1}{f_\pi} |\langle \pi^0 | H_W | K_L \rangle| (1 - m_\pi^2/m_K^2), \\ |\mathcal{M}_{K^+\pi^+\pi^0}^{+0}| &= \frac{1}{2f_\pi} |\langle \pi^+ | H_W | K^+ \rangle + \langle \pi^0 | H_W | K_L \rangle| (1 - m_\pi^2/m_K^2), \end{aligned} \quad (1)$$

where the factor  $(1 - m_\pi^2/m_K^2)$  must be used in Eqs. 1 [3]. Note that the isospin invariance  $\langle \pi^+ | H_W | K^+ \rangle = -\langle \pi^0 | H_W | K_L \rangle$  manifests the  $\Delta I = 1/2$  rule in Eq. 1 with  $|\mathcal{M}^{+-}| = |\mathcal{M}^{00}|$  and  $|\mathcal{M}^{+0}| \rightarrow 0$ , then compatible with data and  $|\mathcal{M}^{+0}| / |\mathcal{M}^{+-}| \approx 0.047$ . However, one must also account for the final-state [FS] interactions with the observed  $\pi\pi$  phase shifts,  $\delta_l^{I\pi\pi}$ , evaluated at the kaon mass,  $\delta_0^0 - \delta_0^2 \approx 45^\circ$  [4]. To do so, the  $K_S \rightarrow \pi\pi$  amplitudes of Eqs. 1 are written as

$$\begin{aligned} \mathcal{M}_{K_S\pi\pi}^{+-} &= a_{1/2} + \frac{2}{3}a_{3/2} \\ \mathcal{M}_{K_S\pi\pi}^{00} &= a_{1/2} - \frac{4}{3}a_{3/2}, \end{aligned} \quad (2)$$

where the subscripts on the real amplitudes  $a_{1/2}$ ,  $a_{3/2}$  refer to the I-spin of  $H_W$ . The amplitudes including FS interactions are then [1]

$$\begin{aligned} |\mathcal{M}_{K_S\pi\pi}^{+-}|_{FS} &= \left[ a_{1/2}^2 + \frac{4}{9}a_{3/2}^2 + \frac{4}{3}a_{1/2}a_{3/2}\cos(\delta_0^0 - \delta_0^2) \right]^{1/2} \\ |\mathcal{M}_{K_S\pi\pi}^{00}|_{FS} &= \left[ a_{1/2}^2 + \frac{16}{9}a_{3/2}^2 - \frac{8}{3}a_{1/2}a_{3/2}\cos(\delta_0^0 - \delta_0^2) \right]^{1/2}. \end{aligned} \quad (3)$$

The experimental rates, from Ref. [2], give amplitudes

$$\begin{aligned} |\mathcal{M}_{K_S\pi\pi}^{+-}|_{\text{PDG}} &= m_{K_S} \left[ 8\pi\Gamma_{+-}^{K_S}/q \right]^{\frac{1}{2}} = (39.1 \pm 0.2) \times 10^{-8} \text{ GeV}, \\ |\mathcal{M}_{K_S\pi\pi}^{00}|_{\text{PDG}} &= m_{K_S} \left[ 16\pi\Gamma_{00}^{K_S}/q \right]^{\frac{1}{2}} = (37.1 \pm 0.1) \times 10^{-8} \text{ GeV}, \\ |\mathcal{M}_{K^+\pi^+\pi^0}^{+0}|_{\text{PDG}} &= m_{K^+} \left[ 8\pi\Gamma_{+0}^{K^+}/q \right]^{\frac{1}{2}} = (1.832 \pm 0.006) \times 10^{-8} \text{ GeV}, \end{aligned} \quad (4)$$

where  $q$  is the magnitude of the relevant decay momentum. These can be substituted in Eqs. 3 yielding the I-spin amplitudes

$$\begin{aligned} a_{1/2} &\approx 38.42 \times 10^{-8} \text{ GeV}, \\ a_{3/2} &\approx 1.43 \times 10^{-8} \text{ GeV}. \end{aligned} \quad (5)$$

These can in turn be used in the CA-PCAC consistency conditions, Eqs. 1, 2, to extract the reduced matrix element  $\langle \pi^+ | H_W | K^+ \rangle$  (or equivalently  $-\langle \pi^0 | H_W | K_L \rangle$ ). For  $\langle \pi^+ | H_W | K^+ \rangle$ , it is necessary to *subtract* off the contribution from the  $W^+$  pole graph of Fig. 1 [5], namely



Figure 1:  $W$  pole graph for the transition  $\langle \pi^+ | H_W | K^+ \rangle$ .

$$| \langle \pi^+ | H_W | K^+ \rangle |_{\text{Wpole}} = (G_F/\sqrt{2})s_1c_1f_\pi f_K m_K^2 = (0.460 \pm 0.006) \times 10^{-8} \text{ GeV}^2 \quad (6)$$

for  $G_F = 11.6639 \times 10^{-6} \text{ GeV}^{-2}$ ,  $f_K \approx 1.22f_\pi$ ,  $f_\pi \approx 93 \text{ MeV}$  and  $s_1c_1 = 0.217 \pm 0.003$  [2]. This leads to the result [6]

$$\begin{aligned} | \langle \pi^+ | H_W | K^+ \rangle | &= ((3.980 \pm 0.020) - (0.460 \pm 0.006)) \times 10^{-8} \text{ GeV}^2 \\ &= (3.520 \pm 0.021) \times 10^{-8} \text{ GeV}^2, \end{aligned} \quad (7)$$

where the first 3.980 number in Eq. 7 stems from Eqs. 1-5,  $| \mathcal{M}_{K_S\pi\pi}^{+-} | \approx 39.373 \times 10^{-8} \text{ GeV}$ . For the matrix element  $\langle \pi^0 | H_W | K_L \rangle$ , for which there is no  $W$  pole term, Eqs. 1-3 give directly

$$| \langle \pi^0 | H_W | K_L \rangle | = (3.666 \pm 0.010) \times 10^{-8} \text{ GeV}^2. \quad (8)$$

It is reassuring that these values in Eqs. 7 and 8 are quite close. Again assuming isospin invariance, we average Eqs. 7 and 8 to find the mean reduced matrix element

$$| \langle \pi^+ | H_W | K^+ \rangle |_{\text{avg}} = | \langle \pi^0 | H_W | K_L \rangle |_{\text{avg}} = (3.637 \pm 0.009) \times 10^{-8} \text{ GeV}^2. \quad (9)$$

## II.2 From $K \rightarrow 3\pi$ decays

Reducing in two pions consistently, the four measured  $K_{3\pi}$  weak decay amplitudes [2]

( $|\mathcal{M}_{++-}^+| = (1.93 \pm 0.01) \times 10^{-6}$ ,  $|\mathcal{M}_{+00}^+| = (0.96 \pm 0.01) \times 10^{-6}$ ,  $|\mathcal{M}_{+0-}^L| = (0.91 \pm 0.01) \times 10^{-6}$ ,  $|\mathcal{M}_{000}^L| = (2.60 \pm 0.02) \times 10^{-6}$ ) predict the CA-PCAC reduced matrix elements [1]:

$$\begin{aligned} |\langle \pi^+ | H_W | K^+ \rangle| &= 2f_\pi^2(1 - m_\pi^2/m_K^2)^{-1} |\langle \pi^+\pi^+\pi^- | H_W | K^+ \rangle| = (3.63 \pm 0.02) \times 10^{-8} \text{ GeV}^2, \\ |\langle \pi^+ | H_W | K^+ \rangle| &= 4f_\pi^2(1 - m_\pi^2/m_K^2)^{-1} |\langle \pi^+\pi^0\pi^0 | H_W | K^+ \rangle| = (3.59 \pm 0.04) \times 10^{-8} \text{ GeV}^2, \\ |\langle \pi^0 | H_W | K_L \rangle| &= 4f_\pi^2(1 - m_\pi^2/m_K^2)^{-1} |\langle \pi^+\pi^0\pi^- | H_W | K_L \rangle| = (3.42 \pm 0.04) \times 10^{-8} \text{ GeV}^2, \\ |\langle \pi^0 | H_W | K_L \rangle| &= \frac{4}{3}f_\pi^2(1 - m_\pi^2/m_K^2)^{-1} |\langle 3\pi^0 | H_W | K_L \rangle| = (3.24 \pm 0.02) \times 10^{-8} \text{ GeV}^2. \end{aligned} \quad (10)$$

Once more assuming isospin invariance, the four reduced  $K \rightarrow \pi$  transitions for  $K_{3\pi}$  decays in Eq. 10 average to

$$|\langle \pi^+ | H_W | K^+ \rangle|_{\text{PCAC}} = |\langle \pi^0 | H_W | K_L \rangle|_{\text{PCAC}} = (3.449 \pm 0.015) \times 10^{-8} \text{ GeV}^2. \quad (11)$$

To show that the final-state-corrected  $K_{2\pi}$  result, Eq. 9 and the nearby PCAC-averaged  $K_{3\pi}$  result, Eq. 11, (where FS interactions are known [4] to be minimal) do indeed refer to the same  $K \rightarrow \pi$  weak transition, we must verify that the PCAC corrections in the two cases are in fact minimal, given the observed rate ratio [2]:

$$\frac{\Gamma(K^+ \rightarrow \pi^+\pi^+\pi^-)}{\Gamma(K_S \rightarrow \pi^+\pi^-)} \Big|_{\text{PDG}} = \frac{(\hbar/\tau_{K^+})(5.59 \pm 0.08)\%}{(\hbar/\tau_{K_S})(68.61 \pm 0.28)\%} = (5.88 \pm 0.09) \times 10^{-4}. \quad (12)$$

This ratio, Eq. 12, must then be compared to the analog PCAC rate ratio, where the PCAC-consistency amplitude ratio [1]  $|A_{++}^+|_{\text{PCAC}} = |\langle \pi^+\pi^- | H_W | K_S \rangle| / 2f_\pi$  generates the rate ratio

$$\frac{\Gamma(K^+ \rightarrow \pi^+\pi^+\pi^-)}{\Gamma(K_S \rightarrow \pi^+\pi^-)} \Big|_{\text{PCAC}} = \frac{0.798 \times 10^{-6} \text{ GeV}}{0.206 \text{ GeV}} \left( \frac{1}{2f_\pi} \right)^2 8\pi m_{K_S}^2 \left( 1 - \frac{m_\pi^2}{m_K^2} \right)^2 \approx 5.94 \times 10^{-4}. \quad (13)$$

Note that the measured rate ratio Eq. 12 is close to the PCAC-consistency ratio Eq. 13. Here, the 3-body phase-space factor  $0.798 \times 10^{-6} \text{ GeV}$  was computed in Ref. [1]. Likewise the rate ratio for  $K_L \rightarrow 3\pi^0/K_S \rightarrow 2\pi^0$  is for the PDG  $(1.16 \pm 0.02) \times 10^{-3}$  and  $1.32 \times 10^{-3}$  for PCAC consistency. The amplitude ratios are even closer. Thus it should not be surprising that the scales of 3.64 in Eq. 9 and 3.45 in Eq. 11 are indeed close.

### II.3 From $K_L \rightarrow 2\gamma$ decays

Low-mass pole diagrams also generate LD weak amplitudes. The  $\pi^0$  pole gives the  $K_L \rightarrow 2\gamma$  amplitude magnitude [2]

$$| \langle 2\gamma | H_W | K_L \rangle | = \frac{|\langle \pi^0 | H_W | K_L \rangle|}{m_{K_L}^2 - m_{\pi^0}^2} F_{\pi^0\gamma\gamma} = (3.49 \pm 0.05) \times 10^{-9} \text{ GeV}^{-1}, \quad (14)$$

where the  $\pi^0\gamma\gamma$  amplitude (either from data or theory) is  $\alpha/\pi f_\pi = 0.025 \text{ GeV}^{-1}$  and we have neglected the Levi-Civita factor on both sides of Eq. 14. This then leads immediately to

$$| \langle \pi^0 | H_W | K_L \rangle |_{\pi^0 \text{ pole}} = (3.20 \pm 0.04) \times 10^{-8} \text{ GeV}^2. \quad (15)$$

The  $\eta$  and  $\eta'$  pole graphs in Fig. 2 have opposite sign. However, they are not quite equal in magnitude and a detailed calculation [6] shows that the  $K \rightarrow \pi$  transition in Eq. 15 is then *effectively enhanced* by 11.1% to

$$| \langle \pi^0 | H_W | K_L \rangle |_{\pi^0, \eta, \eta' \text{ poles}} = (3.56 \pm 0.04) \times 10^{-8} \text{ GeV}^2. \quad (16)$$

#### II.4 From the $K^+ \rightarrow \pi^+ e^+ e^-$ and $K^+ \rightarrow \pi^+ \mu^+ \mu^-$ rare decays

The recent Brookhaven  $K^+ \rightarrow \pi^+ e^+ e^-$  experiment E865 finds the amplitude [7, 8] at  $q^2 = 0$

$$| A(0) |_{K\pi e\bar{e}} = (4.00 \pm 0.18) \times 10^{-9} \text{ GeV}^{-2}. \quad (17)$$

Recently, Burkhardt *et al.* [8] showed that both the decay rate and the  $q^2$  dependence can be well understood in a straightforward model in which the only terms that survive at  $q^2 = 0$  are the LD virtual bremsstrahlung graphs of Fig. 3, which scale with the weak matrix element  $\langle \pi^+ | H_W | K^+ \rangle$  that we study here. These virtual bremsstrahlung graphs predict the long-distance (LD) weak amplitude at  $q^2 = 0$  [8]:

$$| A_{LD}(0) | = e^2 \left| \frac{\langle \pi^+ | H_W | K^+ \rangle}{m_{K^+}^2 - m_{\pi^+}^2} \right| \left| \frac{dF_{\pi^+}}{dq^2} - \frac{dF_{K^+}}{dq^2} \right|, \quad (18)$$

where vector meson dominance (VMD)  $\rho$ ,  $\omega$  and  $\phi$  poles require e.g. the  $\rho$  form factor  $F_{\pi^+}(q^2) = (1 - q^2/m_\rho^2)^{-1}$  and

$$\left. \frac{dF_{\pi^+}}{dq^2} \right|_{q^2=0} = 1/m_\rho^2 = 1.69 \text{ GeV}^{-2}. \quad (19)$$

Likewise, the  $\rho$ ,  $\omega$  and  $\phi$  VMD poles for the  $F_{K^+}(q^2)$  form factor predict [8]

$$\left. \frac{dF_{K^+}}{dq^2} \right|_{q^2=0} = \frac{n_\rho}{m_{\rho^0}^2} + \frac{n_\omega}{m_\omega^2} + \frac{n_\phi}{m_{\phi^0}^2} = 1.42 \text{ GeV}^{-2} \quad (20)$$

as measured from  $\rho, \omega, \phi \rightarrow e^+e^-$  electromagnetic decays. Here,  $6n_{\rho,\omega,\phi} = 1, 3, 2$  from VMD [8, 9] fixing the normalisation  $n_\rho + n_\omega + n_\phi = 1$  as required. Finally, substituting Eqs. 19, 20 into Eq. 18 and using the E865  $K^+ \rightarrow \pi^+e^+e^-$  amplitude in Eq. 17, one extracts the LD transition:

$$\begin{aligned} |\langle \pi^+ | H_W | K^+ \rangle| &= e^{-2} |A(0)|_{K^+ \rightarrow \pi^+e^+e^-} (m_{K^+}^2 - m_{\pi^+}^2) \left| \frac{dF_{\pi^+}}{dq^2} - \frac{dF_{K^+}}{dq^2} \right|_{q^2=0}^{-1} \\ &= (3.62 \pm 0.16) \times 10^{-8} \text{ GeV}^2. \end{aligned} \quad (21)$$

Possible short-distance (SD) corrections to Eq. 21 have been shown to be less than 10% [10], partly because the top quark corrections are small due to the large top-quark mass ( $m_t \sim 175 \text{ MeV}$ ) and also because QCD corrections substantially reduce the SD contribution. This lack of knowledge of the SD contribution is the dominant source of uncertainty in the weak matrix element, so we take the value to be

$$|\langle \pi^+ | H_W | K^+ \rangle| = (3.62 \pm 0.36) \times 10^{-8} \text{ GeV}^2. \quad (22)$$

Eq. 22 is in close agreement with Eqs. 9, 11, 16 above.

Brookhaven experiment E865 has also measured [11] the decay  $K^+ \rightarrow \pi^+\mu^+\mu^-$ . Because of the limited statistics of this measurement, compared to the  $K^+ \rightarrow \pi^+e^+e^-$  channel, an extrapolation quadratic in  $q^2$  gives an unduly large error in the amplitude at  $q^2 = 0$ . Therefore, we invoke lepton universality which implies that the shape of the  $q^2$  dependence of  $A(q^2)$  is the same for these two channels. Thus we fit the amplitude, as a function of  $q^2$ , for  $K^+ \rightarrow \pi^+\mu^+\mu^-$  using the coefficients of  $q^2$  and  $q^4$  determined from the fit [7] to the  $K^+ \rightarrow \pi^+e^+e^-$  data. Again, we allow a contribution of 10% to the error in  $A(0)$  due to the uncertainty in the SD contribution. The result is

$$|A(0)|_{K\pi\mu\bar{\mu}} = (4.45 \pm 0.67) \times 10^{-9} \text{ GeV}^{-2} \quad (23)$$

from which, using Eqs. 18 and 21,

$$|\langle \pi^+ | H_W | K^+ \rangle| = (4.0 \pm 0.6) \times 10^{-8} \text{ GeV}^2. \quad (24)$$

## II.5 Meson weak self-energy graphs

We now compare the five experimental  $\langle \pi | H_W | K \rangle$  LD weak scales in Eqs. 9, 11, 16, 22, 24 (extracted from  $K_{2\pi}$ ,  $K_{3\pi}$ ,  $K_{L2\gamma}$ ,  $K_{\pi^+e^+e^-}^+$ ,  $K_{\pi^+\mu^+\mu^-}^+$  weak decays, averaging to  $3.59 \times 10^{-8}$  GeV<sup>2</sup>) with the theoretical prediction of the “eye diagram” model-independent meson loop graphs of Fig. 4.

This amplitude, which has UV cutoff  $\Lambda \approx 1.87$  GeV near the observed D mass [12], is found *via* a Wick rotation to  $q^2 = -p^2$ ,  $d^4p = i\pi^2 q^2 dq^2$  with  $q^2 = x$  and  $s_1 c_1 = 0.217 \pm 0.003$ :

$$\begin{aligned} |\langle \pi^0 | H_W | K_L \rangle| &= \frac{G_F}{\sqrt{2}} s_1 c_1 (m_D^2 - m_K^2) \int^\Lambda \frac{d^4p}{(2\pi)^4} \frac{p^2}{(p^2 - m_D^2)(p^2 - m_K^2)} \\ &= \frac{G_F V_{ud} V_{us} (m_D^2 - m_K^2)}{\sqrt{2} \times 16\pi^2} \int_0^{\Lambda^2} \frac{x^2 dx}{(x + m_D^2)(x + m_K^2)} \\ &= (3.47 \pm 0.05) \times 10^{-8} \text{ GeV}^2, \end{aligned} \quad (25)$$

where the error is dominated by the uncertainty in  $s_1 c_1$ . This result is in excellent agreeent with the weak LD scales in Eqs. 9, 11, 16, 22, 24 above.

An alternative W-mediated approach which builds in the  $\Delta I = 1/2$  structure follows from the quark-model single-quark-line (SQL)  $s \rightarrow d$  weak transition. With u and c quark intermediate states, the GIM  $K_L \rightarrow \pi^0$  LD transition is [13]

$$|\langle \pi^0 | H_W | K_L \rangle| = \frac{G_F}{\sqrt{2}} \frac{s_1 c_1}{4\pi^2} (m_c^2 - m_u^2) m_K^2 \frac{f_K}{f_\pi} \approx 2.92 \times 10^{-8} \text{ GeV}^2 \quad (26)$$

for  $G_F = 11.6639 \times 10^{-6} \text{ GeV}^{-2}$ ,  $s_1 c_1 \approx 0.217$ ,  $m_c \approx 1.5 \text{ GeV}$ ,  $m_u \approx 0.34 \text{ GeV}$  (for constituent quarks) and  $f_K/f_\pi \approx 1.22$ . Then the predicted Eq. 26 is 82% of Eqs. (9,11,16,22,24) above. When the heavier top-quark intermediate state is included using a “heavy-quark approximation” [14], Eq. 26 becomes closer to the  $K_L \rightarrow \pi^0$  LD transition found throughout sect. II.

### III. FIRST and SECOND ORDER TESTS of the SQL TRANSITION

#### III.1 Quark-model $s \rightarrow d$ first-order weak transition

Alternatively, we study the  $K_L \rightarrow \pi^0$  weak transition at the quark level *via* the (Nambu-Goldstone) tightly bound  $\Delta I = \frac{1}{2}$  quark bubble graph of Fig. 5.

We focus on the  $K_S \rightarrow \pi\pi$  decay rate  $\Gamma_S$ . Firstly, one computes from Fig. 5 [15]

$$|\langle \pi^0 | H_W | K_L \rangle| = 2\beta_W m_{K_L}^2 f_K / f_\pi, \quad (27)$$

where  $\beta_W$  is the dimensionless weak SQL scale. From this, the total width of the  $K_S$  is [15, 16, 17]

$$\Gamma_S \approx \frac{3}{16\pi} \frac{q}{m_K^2} |\mathcal{M}_{K_S\pi\pi}^{00}|^2 \approx 3.61 \beta_W^2 m_K. \quad (28)$$

From Ref. [2], the experimental value of  $\Gamma_S$  is

$$\Gamma_S = (73.67 \pm 0.07) \times 10^{-16} \text{ GeV}. \quad (29)$$

Relating Eqs. 28 and 29 gives the weak SQL scale as

$$|\beta_W| \approx \left[ (73.67 \pm 0.07) \times 10^{-16} / 3.61 \times 0.497672 \right]^{1/2} \sim 6.4 \times 10^{-8}, \quad (30)$$

where 0.497672 GeV is the neutral kaon mass. Substituting the value of  $\beta_W$  from Eq. 30 gives for the weak matrix element (see the second reference in [8])

$$|\langle \pi^0 | H_W | K_L \rangle| \sim 3.9 \times 10^{-8} \text{ GeV}^2. \quad (31)$$

This global estimate is compatible with the experimental values found in sect. II. We therefore extend the concept of fig. 5 to the second-order weak process,  $\Delta m_{LS} = m_{K_L} - m_{K_S}$ .

### III.2 Quark model $s \rightarrow d$ second-order weak transition and the $K_L - K_S$ mass difference $\Delta m_{LS}$

Since  $\Delta m_{LS}$  can be taken as a *second-order weak transition*, one may express the data as [2, 18]

$$\Delta m_{LS} = (0.4736 \pm 0.0012) \Gamma_S, \text{ or equivalently} \quad (32)$$

$$\Delta m_{LS} = (0.7011 \pm 0.0016) \times 10^{-14} m_K, \quad (33)$$

in order to find a more accurate value for the weak SQL scale  $\beta_W$  and a further value for  $|\langle \pi^0 | H_W | K_L \rangle|$ .

Specifically, the second-order weak quark bubble graph of Fig. 6 (not the usual parameter-dependent W-W quark box) is the obvious generalisation of the first-order weak quark bubble graph of Fig. 5. In both cases the linear- $\sigma$ -model inspired (with PCAC-compatible [19]) pseudoscalar couplings are used. Then the (CP-conserving)  $K^0 - \bar{K}^0$  mixing matrix is diagonalised as

$$\begin{pmatrix} m_{K^0}^2 & \lambda \\ \lambda & m_{\bar{K}^0}^2 \end{pmatrix} \xrightarrow{\phi} \begin{pmatrix} m_{K_S}^2 & 0 \\ 0 & m_{K_L}^2 \end{pmatrix}, \quad (34)$$

with  $\phi = 45^\circ$  for states  $\sqrt{2} |K_{L,S}\rangle = |K^0\rangle \pm |\bar{K}^0\rangle$ . Saturating  $\lambda = \langle K^0 | H_W^{(2)} | \bar{K}^0 \rangle$  via unitarity for the overwhelmingly dominant  $2\pi$  intermediate state [18] predicts  $\phi = \arctan 2\Delta m_{LS}/\Gamma_S \approx \pi/4$ , which in turn gives  $\Delta m_{LS} \approx \Gamma_S/2$ , close to the measured value in Eq. 32.



For the above consistent picture (Figs. 5, 6), ordinary two-level quantum mechanics (independent of quantum field theory) then requires [20]

$$\sin 2\phi = 2\lambda(m_{K_L}^2 - m_{K_S}^2)^{-1} \approx \lambda/m_K \Delta m_{LS}, \quad (35)$$

where the LHS of Eq. 35 is unity for  $\phi = 45^\circ$  (and very nearly unity when CP-violating effects are included) so that

$$\lambda \approx m_K \Delta m_{LS}. \quad (36)$$

However, the off-diagonal matrix element  $\lambda$  in Eqs. 35, 36 also gives from Fig. 6

$$\lambda = \langle K^0 | H_W^{(2)} | \bar{K}^0 \rangle \approx 2\beta_W^2 m_K^2, \quad (37)$$

since the only mass scale in Eq. 37 is  $m_K^2$ , the diagonalisation is second-order weak (requiring a  $\beta_W^2$  factor) and the factor of 2 in Eqs. 27, 37 stems from  $(1 - \gamma_5)^2 = 2(1 - \gamma_5)$ . Standard CA-PCAC considerations [20] also recover Eq. 37.

Combining Eqs. 36, 37 leads to the result

$$\Delta m_{LS} \approx 2\beta_W^2 m_K, \quad (38)$$

which, together with the  $\Delta m_{LS}$  value [2] in Eq. 33, predicts the weak SQL scale

$$|\beta_W| = [(0.7011 \pm 0.0016) \times 10^{-14}/2]^{1/2} \approx (5.921 \pm 0.007) \times 10^{-8}, \quad (39)$$

which gives, with Eq. 27,

$$|\langle \pi^0 | H_W | K_L \rangle| = (3.578 \pm 0.004) \times 10^{-8} \text{ GeV}^2, \quad (40)$$

again compatible with the experimental values found in sect. II.

#### IV. PCAC SPIN-3/2 TESTS of the LD-SQL TRANSITION for $\langle \Xi | H_W | \Omega \rangle$

Another SQL test relates to the decuplet weak decay amplitude  $\Omega^- \rightarrow \Xi^0 \pi^-$  relative to the Rarita-Schwinger transition  $\langle \Xi^- | H_W | \Omega^- \rangle \approx h_2 \bar{u}(\Xi) p^\mu u(\Omega)_\mu$ , but first we extract this latter weak scale from the  $K^0$  tadpole SQL graph of fig. 7 [21] with kaon PCAC strong coupling [22]  $\langle K^0 \Xi^- | \Omega^- \rangle \rightarrow g_2 \rightarrow \sqrt{2}/f_K$ :

$$\begin{aligned}
| \langle \Xi^- | H_W | \Omega^- \rangle | \rightarrow | h_2 | &= | \langle 0 | H_W | K^0 \rangle g_2 | / m_K^2 \\
&\approx | 2\sqrt{2} f_K m_K^2 \beta_W \times \sqrt{2} / f_K m_K^2 | = 4 | \beta_W | .
\end{aligned} \tag{41}$$

However, kaon PCAC is known to be accurate only to within 25 - 30%, so instead we employ strong decuplet-octet baryon-pseudoscalar meson (DBP) data to extract [22]  $g_{DPB} = (m_D + m_B)g_2/2 \approx 15.7$  which is a 20% lower estimate than used for  $g_2$  in Eq. 41. Thus a more accurate estimate for  $h_2$  than Eq. 41 is

$$| h_2 | = | 4\beta_W | / 1.2 \approx 3.3 | \beta_W | . \tag{42}$$

We note that Eq. 42 is quite close to the standard decuplet-octet baryon SU(3) flavour SQL estimate

$$| h_2 | = 3 | \beta_W | \tag{43}$$

for  $\Omega$  constructed from 3 strange quarks. This too can be verified from magnetic-moment data [2], giving the ratio

$$\frac{\mu_\Omega}{\mu_\Lambda} = \frac{(2.02 \pm 0.05)\mu_N}{(0.613 \pm 0.004)\mu_N} = 3.3 \pm 0.1, \tag{44}$$

so we consistently invoke the SU(3) value to compute the weak SQL scale Eq. 43, not Eq. 41, and use the difference between Eqs. 42 and 43 to give a feel for the error.

Returning to  $\Omega^- \rightarrow \Xi^0 \pi^-$  weak decay, we next extract the dominant parity-conserving amplitude  $E$  from experiment [2, 23] with cm momentum  $p = 294$  MeV/c:

$$| E(\Omega^- \rightarrow \Xi^0 \pi^-) | = \frac{m_\Omega}{m_\Omega + m_\Xi} \left[ 24\pi \Gamma_{\Omega\Xi\pi} / p^3 \right]^{1/2} = (1.33 \pm 0.02) \times 10^{-6} \text{ GeV}^{-1}. \tag{45}$$

This observed amplitude in Eq. 45 has remained unaltered for over a decade [21, 23]. It then predicts from pion PCAC (recall the PCAC structures of Eqs. 1)

$$\left| \frac{\langle \Xi^0 \pi^- | H_W | \Omega^- \rangle}{\langle \Xi^- | H_W | \Omega^- \rangle} \right| = \left| \frac{E(\Omega^- \Xi^0 \pi^-)}{h_2} \right| \approx \frac{1}{\sqrt{2} f_\pi} \text{ or } | h_2 | \approx 17.5 \times 10^{-8}. \tag{46}$$

This estimate Eq. 46 is further supported using SU(6) Thirring product wave functions [21, 23]. Finally, we use Eqs. 43, 46 to provide the third determination of the SQL scale  $\beta_W$ :

$$| \beta_W | = | h_2 | / 3 \approx 17.5 \times 10^{-8} / 3 = (5.8 \pm 0.6) \times 10^{-8}, \quad (47)$$

reasonably near the prior estimates of Eqs. 30, 39. As mentioned above, the error quoted reflects the consistency indicated by the difference between Eqs. 42 and 43. This gives, with Eq. 27,

$$| \langle \pi^0 | H_W | K_L \rangle | = 2\beta_W m_{K_L}^2 f_K / f_\pi = (3.5 \pm 0.4) \times 10^{-8} \text{ GeV}^2, \quad (48)$$

again compatible with the experimental values found in sect. II.

## V. DOMINANT LD $K_L \rightarrow \mu\bar{\mu}$ DECAY

The dominant first-order weak LD  $\pi^0$  and  $\eta$  poles are displayed in Figs. 8(a), 8(b) while the (smaller) second-order weak short-distance (SD) graph is shown in Fig. 8(c). First from  $\pi^0 \rightarrow e\bar{e}$ ,  $\eta \rightarrow \mu\bar{\mu}$ ,  $K_L \rightarrow \mu\bar{\mu}$  decay data we extract the various dimensionless amplitudes defined from an S-matrix element  $S_{fi} = F(Pl\bar{l})\bar{u}i\gamma_5 v\bar{\delta}^4(p_f - p_i)$  with lepton spinors normalised covariantly, generating decay rates  $\Gamma(Pl\bar{l}) = p | F(Pl\bar{l}) |^2 / 4\pi$  for cm momenta  $p = 67 \text{ MeV}/c$ ,  $252 \text{ MeV}/c$ ,  $225 \text{ MeV}/c$  for  $\pi^0 \rightarrow e\bar{e}$ ,  $\eta \rightarrow \mu\bar{\mu}$ ,  $K_L \rightarrow \mu\bar{\mu}$  respectively. The PDG tables [2] then require the central value amplitude magnitudes to be:

$$\begin{aligned} | F(\pi^0 e\bar{e}) | &= (3.02 \pm 0.33) \times 10^{-7}, \\ | F(\eta \mu\bar{\mu}) | &= (1.85 \pm 0.31) \times 10^{-5}, \\ | F(K_L \mu\bar{\mu}) | &= (2.26 \pm 0.05) \times 10^{-12}. \end{aligned} \quad (49)$$

While the  $\pi e\bar{e}$  and  $\eta \mu\bar{\mu}$  amplitudes in Eq. 49 are of electromagnetic origin [24, 25], it is clear that the much smaller  $K_L \mu\bar{\mu}$  amplitude in Eq. 49 is a weak decay suppressed by  $10^{-7}$ .

In order to apply the observed amplitudes of Eq. 49 to the graph of Fig. 8(a), we must first scale up the  $\pi^0 e\bar{e}$  amplitude to the  $\pi^0 \mu\bar{\mu}$  *via* one power of lepton mass (no covariant normalisation)  $m_\mu/m_e \approx 206.77$  to

$$| F(\pi^0 \mu\bar{\mu}) | = 206.77 \times 3.02 \times 10^{-7} = (6.24 \pm 0.68) \times 10^{-5}. \quad (50)$$

Then the sum of the graphs Figs. 8(a),(b) predicts the weak amplitude magnitude

$$\begin{aligned} | F(K_L \mu\bar{\mu}) | &= \left| \frac{\langle \pi^0 | H_W | K_L \rangle F(\pi^0 \mu\bar{\mu})}{m_K^2 - m_\pi^2} + \frac{\langle \eta | H_W | K_L \rangle F(\eta \mu\bar{\mu})}{m_K^2 - m_\eta^2} \right| \\ &\approx (9.74 - 7.37) \times 10^{-12} = (2.4 \pm 1.6) \times 10^{-12}. \end{aligned} \quad (51)$$

Here we have taken  $\langle \pi^0 | H_W | K_L \rangle \approx 3.58 \times 10^{-8} \text{ GeV}^2$  as the average LD weak scale in Sec. II and also divided by  $\sqrt{3}$  in  $\langle \eta | H_W | K_L \rangle$  using SU(3) symmetry for  $\eta = \eta_8$  since  $d_{866}/d_{366} = 1/\sqrt{3}$ . We find it significant that the simple estimate in Eq. 51 is so close to  $K_L \mu \bar{\mu}$  data  $2.26 \times 10^{-12}$  in Eq. 49. Prior studies used complex two-loop graphs and  $\gamma\gamma$  unitarity integrals, but still ended up with a result near Eq. 51 anyway [24, 25].

Alternatively, we could input the experimental value of the  $K_L \rightarrow \mu \bar{\mu}$  amplitude,  $(2.26 \pm 0.05) \times 10^{-12}$ . If we assume the SU(3) value for  $\eta = \eta_8$  of  $1/\sqrt{3}$  for the ratio  $\langle \eta | H_W | K_L \rangle / \langle \pi^0 | H_W | K_L \rangle$ , we can solve Eq. 51 for the weak matrix element, giving

$$| \langle \pi^0 | H_W | K_L \rangle | = (3.4 \pm 2.4) \times 10^{-8} \text{ GeV}^2. \quad (52)$$

Given the 75% cancellation between the  $\pi^0$  and  $\eta$  poles in Eq. 51, we must verify that this net LD amplitude is still larger than the second-order weak SD amplitude of Fig. 8(c). The latter SD box graph [26] is driven by the heavy t quark at  $m_t \sim 175 \text{ GeV}$  or  $X_t = m_t^2/m_W^2 \approx 4.8$  with

$$G(X_t) = \frac{3}{4} \left[ \frac{X_t}{X_t - 1} \right]^2 \ln X_t + \frac{X_t}{4} + \frac{3}{4} \frac{X_t}{1 - X_t} \sim 2, \quad (53)$$

then predicting the SD amplitude

$$| F_{K_L \mu \bar{\mu}}^{SD} | \sim s_1 c_1 s_2^2 \times 10^{-9} G(X_t) \sim 2 \times 10^{-13} \quad (54)$$

for  $s_1 c_1 \sim 0.22$ ,  $s_2 \sim 0.02$ . The ratio of Eq. 51 to Eq. 54 then suggests

$$| F^{LD} / F^{SD} |_{K_L \mu \bar{\mu}} \sim 23.7/2 \sim 12, \quad (55)$$

so indeed the LD amplitude is more than an order of magnitude greater than the  $K_L \rightarrow \mu \bar{\mu}$  SD amplitude.

## VI. LD $K_S \rightarrow 2\gamma$ WEAK DECAY

Finally, we consider the parity-violating (PV) weak decay  $K_S \rightarrow 2\gamma$ . Note that the relative errors are significantly larger than for the parity-conserving (PC) weak decay  $K_L \rightarrow 2\gamma$ , i.e. with observed amplitude magnitudes [2, 6] found from  $\Gamma(K\gamma\gamma) = m_K^3 | F_{K\gamma\gamma} |^2 / 64\pi$ :

$$| F_{K_L \gamma \gamma} | = (3.49 \pm 0.05) \times 10^{-9} \text{ GeV}^{-1}, \quad | F_{K_S \gamma \gamma} | = (5.4 \pm 1.0) \times 10^{-9} \text{ GeV}^{-1}, \quad (56)$$

with both amplitudes scaled to the Levi-Civita  $\epsilon$  factor.

Given the  $\pi^0$  and  $\sigma$  pole graphs of Figs. 2 and 9, the corresponding Feynman amplitude magnitudes are

$$|\langle 2\gamma | H_W^{PC} | K_L \rangle| = \left| \frac{\langle \pi^0 | H_W^{PC} | K_L \rangle}{m_K^2 - m_{\pi^0}^2} F_{\pi^0 2\gamma} \right| \approx 3.49 \times 10^{-9} \text{ GeV}^{-1}, \quad (57)$$

$$|\langle 2\gamma | H_W^{PV} | K_S \rangle| = \left| \frac{\langle \sigma | H_W^{PV} | K_S \rangle}{m_K^2 - m_\sigma^2 + im_\sigma \Gamma_\sigma} \right| |F_{\sigma 2\gamma}| \sim 5.4 \times 10^{-9} \text{ GeV}^{-1}. \quad (58)$$

Although the  $\pi^0 \rightarrow 2\gamma$  amplitude is actually measured as  $(0.025 \pm 0.001) \text{ GeV}^{-1}$  (in agreement with the PVV quark graph or the AVV anomaly  $\alpha/\pi f_\pi = 0.025 \text{ GeV}^{-1}$  with rate  $\Gamma_{\pi^0 \gamma\gamma} = m_\pi^3 |F_{\pi^0 \gamma\gamma}|^2 / 64\pi$ ), neither the broad  $\sigma$  mass-width nor the  $\sigma \rightarrow 2\gamma$  decay rate is accurately known.

Taking  $\Gamma_\sigma \sim m_\sigma$  along with the (reasonable) chiral value [6]

$$|\langle \sigma | H_W^{PV} | K_S \rangle| = |\langle \pi^0 | H_W^{PC} | K_L \rangle| \approx 3.58 \times 10^{-8} \text{ GeV}^2 \quad (59)$$

as found in Sec. II, the estimate [27]  $\Gamma_{\sigma\gamma\gamma} = (3.8 \pm 1.5) \text{ keV}$  along with the analogue rate  $\Gamma_{\sigma\gamma\gamma} = m_\sigma^3 |F_{\sigma\gamma\gamma}|^2 / 64\pi$  and Eq. 58 in turn requires the central value of the  $\sigma$  mass and the  $\sigma \rightarrow \gamma\gamma$  amplitude to be (*without* making any theoretical assumptions)

$$m_\sigma \approx 614 \text{ MeV}, \quad |F_{\sigma\gamma\gamma}| \approx 2.3\alpha/\pi f_\pi \approx 0.057 \text{ GeV}^{-1}. \quad (60)$$

From a phenomenological viewpoint, a 614 MeV  $\sigma$  mass is near the central mass now listed in the PDG tables [2],  $m_\sigma = 400 - 1200 \text{ MeV}$ , also close to the E791 collaboration [28] weak decay analysis,  $m_\sigma \sim 500 \text{ MeV}$ . Moreover, the  $|F_{\sigma\gamma\gamma}| \sim 2.3\alpha/\pi f_\pi$  amplitude value is near the constituent-quark-model value of  $(\frac{4}{9} + \frac{1}{9})N_c\alpha/\pi f_\pi = (5/3)\alpha/\pi f_\pi$  enhanced by 30% due to meson  $\pi^+$  and  $K^+$  loops to  $2.2\alpha/\pi f_\pi$  [6]. It is satisfying that Eqs. 60 (resulting from Eqs. 56 - 59) are so close to these experimental and theoretical values.

We end this  $\sigma$ -dominated  $K_S \rightarrow 2\gamma$  section by including the  $\sigma$ -dominated  $K_L \rightarrow \pi^0 2\gamma$  rate. Folding in the latter 3-body phase space integral from Ref. [29] of  $1.7 \times 10^{-4} \text{ GeV}^4$ , the PCAC rate ratio is predicted to be

$$\frac{\Gamma(K_L \rightarrow \pi^0 2\gamma)}{\Gamma(K_S \rightarrow 2\gamma)} \Big|_{PCAC} = \frac{(m_\sigma \Gamma_\sigma)^2 (1.7 \times 10^{-4} \text{ GeV}^4)}{m_K^6 (4\pi f_\pi)^2} = 11.6 \times 10^{-4} \quad (61)$$

given  $f_\pi = 93 \text{ MeV}$ , for  $m_\sigma = \Gamma_\sigma = 614 \text{ MeV}$  from Eq. 60, close to the measured PDG rate ratio [2, 6]

$$\frac{\Gamma(K_L \rightarrow \pi^0 2\gamma)}{\Gamma(K_S \rightarrow 2\gamma)} \Big|_{PDG} = \frac{(\hbar/\tau_L)(1.68 \pm 0.10) \times 10^{-6}}{(\hbar/\tau_S)(2.4 \pm 0.9) \times 10^{-6}} = (12.1 \pm 4.6) \times 10^{-4}, \quad (62)$$

Source		Value (in units of $10^{-8} \text{ GeV}^2$ )
$K_S \rightarrow 2\pi$	Expt	$3.637 \pm 0.009$
$K \rightarrow 3\pi$	Expt	$3.449 \pm 0.015$
$K_L \rightarrow 2\gamma$	Expt	$3.56 \pm 0.04$
$K^+ \rightarrow \pi^+ e^+ e^-$	Expt	$3.62 \pm 0.36$
$K^+ \rightarrow \pi^+ \mu^+ \mu^-$	Expt	$4.0 \pm 0.6$
$K_L \rightarrow \mu^+ \mu^-$	Expt	$3.4 \pm 2.4$
$\Omega^- \rightarrow \Xi\pi$	Expt	$3.5 \pm 0.4$
Second-order weak SQL $\Delta m_{LS}$	Theory	$3.578 \pm 0.004$
W-mediated self-energy graphs	Theory	$3.47 \pm 0.05$

Table 1: Values derived for the  $K \rightarrow \pi$  matrix element magnitude.

for the observed lifetimes  $\tau_L = (5.17 \pm 0.04) \times 10^{-8} \text{sec}$ ,  $\tau_S = (0.8935 \pm 0.0008) \times 10^{-10} \text{sec}$ . Note that the weak scale  $\langle \sigma | H_W^{PV} | K_S \rangle$  divides out of the PCAC ratio Eq. 61. Yet the nearness of Eqs. 61, 62 gives further PCAC support for the  $K_S \rightarrow 2\pi$  and  $K_L \rightarrow 3\pi$  PCAC  $K \rightarrow \pi$  transition in Sect. II.

## VII. CONCLUSION

In Sec.II we showed that the measured decay rates for  $K_S \rightarrow 2\pi$ ,  $K \rightarrow 3\pi$ ,  $K_L \rightarrow 2\gamma$ ,  $K^+ \rightarrow \pi^+ e \bar{e}$ ,  $K^+ \rightarrow \pi^+ \mu \bar{\mu}$  lead to the average long distance (LD) weak scale  $|\langle \pi | H_W | K \rangle|$  and also derive a theoretical estimate for this quantity. Then in Sec.III we computed the single quark line (SQL) s $\rightarrow$ d dimensionless weak scale  $|\beta_W|$  from both first-order and second-order weak transitions. In Sec.IV we verified the above weak scales by reviewing the observed spin 3/2  $\Omega^- \rightarrow \Xi^0 \pi^-$  weak decays and in Sec.V we computed LD and SD  $K_L \rightarrow \mu \bar{\mu}$  weak decay amplitudes. Finally in Sec VI we studied LD  $K_S \rightarrow 2\gamma$  weak decay and its PCAC extension to  $K_L \rightarrow \pi^0 2\gamma$ .

All of these estimates give strikingly similar values for the weak  $K \rightarrow \pi$  matrix element (without any arbitrary parameters). Table 1 summarises the results. The average of the seven experimental values (derived from eleven measured rates) in Table 1 is

$$|\langle \pi^+ | H_W | K^+ \rangle| = |\langle \pi^0 | H_W | K_L \rangle| = (3.59 \pm 0.05) \times 10^{-8} \text{ GeV}^2, \quad (63)$$

where the error quoted is the external error.

The errors quoted in Table 1 result mostly from propagation of the experimental errors on the input data and, apart from a few cases, do not include any contribution from the uncertainty in the theoretical methods. An estimate of the reliability of the procedures used here is provided by the external error on the seven experimental values in Table 1. The fact that this external error, quoted in Eq. 63, is just 1.4% supports the overall consistency of the methods used and therefore

the reliability of our numerical value for the  $K \rightarrow \pi$  weak matrix element. It is also noteworthy that the experimental result in Eq. 63 is in excellent agreement with the mean of the theoretical estimates in Table 1, which is  $(3.577 \pm 0.004) \times 10^{-8} \text{ GeV}^2$ .

## ACKNOWLEDGEMENTS

We are grateful to G. Eilam, V. Elias and B. Bassalleck for many discussions. We acknowledge support from the US DOE.

## References

- [1] R.E. Karlsen and M.D. Scadron, Phys. Rev. D **45**, 4108 (1992).
- [2] Particle Data Group, D.E. Groom *et al.*, Eur. Phys. J. **C15**, 1 (2000). On p. 110, we use the CKM central value  $s_1 c_1 = V_{ud} V_{us} = (0.9750 \pm 0.0008) \times (0.2225 \pm 0.0035) = 0.217 \pm 0.003$ .
- [3] N. Cabibbo, Phys. Rev. Lett. **12**, 62 (1964); M. Gell-Mann, *ibid.* **12**, 155 (1964).
- [4] G. Grayer *et al.*, Nucl. Phys. **B75**, 189 (1974); N. Durusoy *et al.*, Phys. Lett. **B45**, 517 (1973). For a more recent summary of experimental  $\pi\pi$  phase shifts, see J. Gasser and Ulf-G. Meissner, Phys. Lett. **B258**, 219 (1991).
- [5] The  $W$  pole term was added rather than subtracted from  $\langle \pi^+ | H_W | K^+ \rangle$  in Ref. [1].
- [6] Footprints of a broad  $\sigma(500-600)$  in weak interaction processes, A.D. Polosa, N.A. Tornquist, M.D. Scadron and V. Elias, hep-ph/0005106; Mod. Phys. Lett. **A17**, 569 (2002).
- [7] R. Appel *et al.* (E865 collaboration), Phys. Rev. Lett. **83**, 4482 (1999).
- [8] H. Burkhardt *et al.*, Phys. Lett. **B512**, 317 (2001); also see G. Eilam and M.D. Scadron, Phys. Rev. **D31**, 2263 (1985).
- [9] C. Ayala and A. Bramon, Europhys. Lett. **4**, 777 (1987). Actually, we extract  $6n_{\rho,\omega,\phi} = 0.94, 3.08, 1.99$  directly from  $e\bar{e}$  weak decays so that the normalisation is  $n_\rho + n_\omega + n_\phi = 1.0017$ , very close to unity as demanded.
- [10] C.O. Dib, I. Dunietz and F.J. Gilman, Phys. Rev. **D39**, 2639 (1989).
- [11] H. Ma *et al.*, hep-ex/9910047; Phys. Rev. Lett. **84**, 2580 (2000).
- [12] R.E. Karlsen and M.D. Scadron, Mod. Phys. Lett. **A6**, 543 (1991).

- [13] R. Delbourgo and M.D. Scadron, *Nuovo Cimento Lett.* **44**, 193 (1985)
- [14] R. Delbourgo and D. Liu, *Aust. J. Phys.* **53**, 737 (2000); hep-ph/0010155.
- [15] The soft pion theorem applied to the momentum (axial-vector) divergence requires on the kaon mass shell  $q \cdot M = if_\pi \langle \pi^0 | H_W | K_L \rangle = i2\beta_W f_K m_K^2$ . This recovers eq. (27). Also see J. Cronin, *Phys. Rev.* **161**, 1483 (1967) eq. (48).
- [16] For light plane-damped wave functions see N.H. Fuchs and M.D. Scadron, *Nuovo Cimento* **A93**, 205 (1986); C. Michael and C. Payne, *Nucl. Phys.* **B148**, 102 (1979); *Phys. Lett.* **B91**, 41 (1980). We drop the factor of 0.97 from these papers.
- [17] R. Delbourgo and M.D. Scadron, *Nuovo Cimento Lett.* **44**, 193 (1985) in eq. (7c) called this SQL scale  $b$  (rather than  $\beta_W$ , our present notation).
- [18] See e.g. R. Marshak, Riazuddin and C. Ryan, *Theory of Weak-Interaction Particle Physics*, (Wiley, NY, 1969) p. 641.
- [19] M. Gell-Mann and M. Levy, *Nuovo Cimento* **16**, 705 (1960); R. Delbourgo and M.D. Scadron, *Mod. Phys. Lett.* **A10**, 251 (1995).
- [20] V. Elias and M.D. Scadron, *Mod. Phys. Lett.* **A10**, 1159 (1995); S.R. Choudhury and M.D. Scadron, *Phys. Rev. D* **53**, 2421 (1996).
- [21] T. Uppal *et al.*, *J. Phys. G* **21**, 621 (1995); S.R. Choudhury and M.D. Scadron, *Phys. Rev. D* **53**, 2421 (1996).
- [22] M.D. Scadron and L.R. Thebaud, *Phys. Rev. D* **8**, 2190 (1973); M.D. Scadron and D. Tadic, *J. Phys. G* **27**, 163 (2001).
- [23] M.D. Scadron and M. Visinescu, *Phys. Rev. D* **28**, 1117 (1983); M.P. Khanna *et al.*, *J. Phys. G* **12**, 1323 (1986).
- [24] See e.g. S. Drell, *Nuovo Cimento* **11**, 692 (1959); M. Berman and D. Geffen, *ibid* **18**, 1192 (1960); L. Sehgal, *ibid* **45**, 785 (1966).
- [25] M.D. Scadron and M. Visinescu, *Phys. Rev. D* **29**, 911 (1984).
- [26] F. Inami and C. Lim, *Prog. Theor. Phys.* **65**, 297 (1981).
- [27] J.M. Boglione and M. Pennington, *Eur. Phys. J. C* **9**, 11 (1999).
- [28] E. Aitala *et al.* (E791 collaboration), *Phys. Rev. Lett.* **86**, 770 (2001); hep-ex/0007028.
- [29] R.E. Karlsen and M.D. Scadron, *Nuovo Cimento* **A106**, 113 (1993).



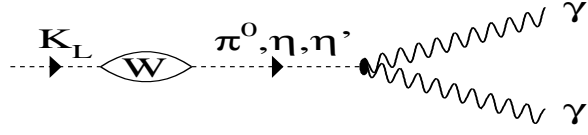


Figure 2: Meson  $\pi^0, \eta, \eta'$  pole graphs for the  $K_L \rightarrow 2\gamma$  decay.

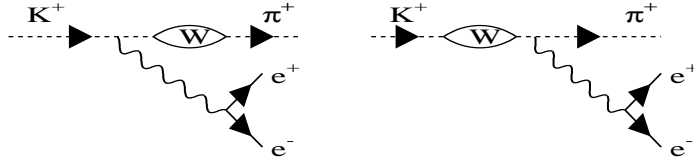


Figure 3: Virtual bremsstrahlung graphs for  $K^+ \rightarrow \pi^+ e^+ e^-$  decay.

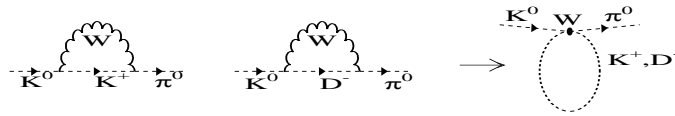


Figure 4: Meson  $W$ -mediated self-energy type graphs for the  $\langle \pi^0 | H_W | K^0 \rangle$  transition.

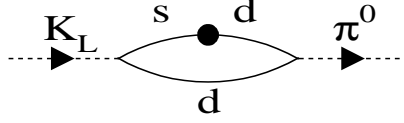


Figure 5: *Quark-model  $s \rightarrow d$  first-order weak transition characterising  $\langle \pi^0 | H_W | K_L \rangle$ .*

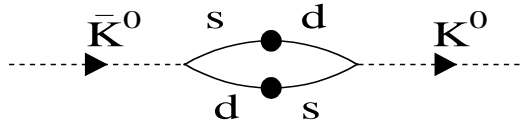


Figure 6: *Quark-model  $s \rightarrow d$  second-order weak transition characterising  $\lambda = \langle K^0 | H_W | \bar{K}^0 \rangle$ .*

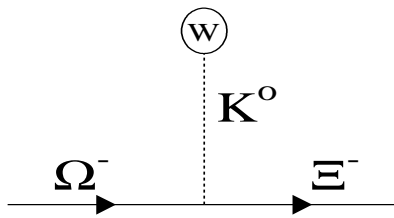


Figure 7: *Kaon tadpole graph characterising  $\langle \Xi^- | H_W | \Omega^- \rangle$ .*

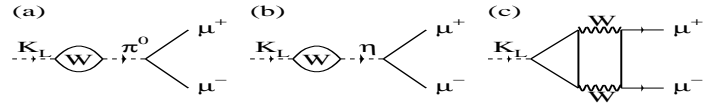


Figure 8: *Weak decay graphs for  $K_L \rightarrow \mu\bar{\mu}$ : (a) LD  $\pi^0$  pole, (b) LD  $\eta$  pole, (c) SD weak box.*

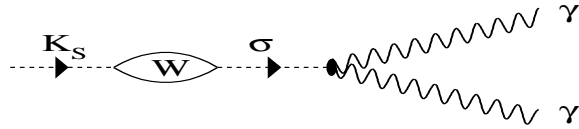


Figure 9:  *$\sigma$  pole for  $K_S$  decay.*